nature immunology

Diversification of TAM receptor tyrosine kinase function

Anna Zagórska[1], Paqui G Través[1], Erin D Lew[1], Ian Dransfield[2] & Greg Lemke[1,3]

The clearance of apoptotic cells is critical for both tissue homeostasis and the resolution of inflammation. We found that the TAM receptor tyrosine kinases Axl and Mer had distinct roles as phagocytic receptors in these two settings, in which they exhibited divergent expression, regulation and activity. Mer acted as a tolerogenic receptor in resting macrophages and during immunosuppression. In contrast, Axl was an inflammatory response receptor whose expression was induced by proinflammatory stimuli. Axl and Mer differed in their ligand specificities, ligand-receptor complex formation in tissues, and receptor shedding upon activation. These differences notwithstanding, phagocytosis by either protein was strictly dependent on receptor activation triggered by bridging of TAM receptor–ligand complexes to the 'eat-me' signal phosphatidylserine on the surface of apoptotic cells.

Billions of apoptotic cells are generated each day in the body's tissues, and the rapid clearance of these dead cells is essential for both tissue homeostasis and resolution of the inflammatory response to infection. Inefficient clearance can lead to tissue damage and the development of autoimmunity[1]. However, the mechanisms responsible for the clearance of apoptotic cells in inflammatory settings versus homeostatic settings are unknown. We sought to determine whether individual members of the TAM family of receptor tyrosine kinases (RTKs)—TYRO3, Axl and Mer[2]—might be specialized to function in these very different environments.

The TAM RTKs are known to regulate the innate immune response[3–5], mediate the homeostatic phagocytosis of apoptotic cells and membranes in adult tissues[6–9], facilitate the infection of target cells by enveloped viruses[10,11] and contribute to the progression and metastasis of human cancers[12–14]. However, the specific roles of individual TAM receptors, together with their ligands GAS-6 and protein S, are poorly understood.

Genetic studies have shown that TAM signaling has an especially important role in sentinel cells of the immune system[3,4], where the principal TAM receptors are Axl and Mer. Activation of either Mer or Axl in these cells has been found to dampen activation of the immune system[3], and the upregulation and activation of Axl in dendritic cells (DCs) is an intrinsic negative feedback inhibitor of the innate immune response[5,15]. Accordingly, deficiencies in TAM signaling result in profound autoimmunity[3,4].

We found that Axl and Mer were dedicated to function in inflammatory and tolerogenic settings, respectively. Macrophage expression of Mer was upregulated by immunosuppressive agents such as dexamethasone (Dex), whereas Axl was inhibited by such agents. Conversely, proinflammatory agents upregulated expression of Axl and inhibited expression of Mer. We found that Mer and Axl specifically mediated the phagocytosis of apoptotic cells in homeostatic environments and inflammatory environments, respectively, and that catalytic activation of these receptors was required for these events. Notably, this activation had to be induced by a TAM ligand whose binding bridged a phagocyte TAM receptor to the 'eat-me' signal phosphatidylserine (PtdSer) on the target apoptotic cell.

We further demonstrated a difference between Mer and Axl in their ligand dependence: both GAS-6 and protein S drove Mer-dependent phagocytosis, but only GAS-6 was able to drive Axl-dependent phagocytosis. GAS-6 was constitutively prebound to Axl in tissues *in vivo* without substantial activation of the receptor, and the presence of GAS-6 in these tissues was dependent on the coexpression of Axl but was independent of Mer and TYRO3. Finally, activation-induced proteolytic cleavage of the extracellular domain of Axl liberated Axl–GAS-6 complexes, which resulted in the rapid removal of both receptor and ligand from tissues. These features of TAM biology must be taken into account in the design and application of any TAM-targeted therapy.

RESULTS

Differences in the expression of Axl and Mer

We analyzed TAM expression in both mouse bone marrow–derived macrophages (BMDMs) and dendritic cells (BMDCs) *in vitro*, and in subsets of cells of the immune system *in vivo*. In BMDCs, prepared with the growth factor GM-CSF[16], Axl had far more abundant expression than that of Mer (**Fig. 1a**). These cultures also had low expression of TYRO3. In contrast, BMDMs had abundant expression of Mer, minimal expression of Axl and no expression of TYRO3 (**Fig. 1a**). The *Axl* mRNA copy number (per nanogram of total RNA ± s.d.) was 29 ± 4 and 28 ± 9 in BMDC cultures and BMDM cultures, respectively, which suggested that most of the difference between these cells was post-transcriptional; in contrast, for *Mertk* mRNA, these numbers were 3 ± 1 and 37 ± 6, respectively. Tyrosine autophosphorylation of Mer was stimulated by both protein S and GAS-6, but Axl was activated only by GAS-6 (**Fig. 1b**).

In vivo, we observed several tissues in which the expression patterns of Axl and Mer paralleled those of cultured macrophages and

[1]Molecular Neurobiology Laboratory, Salk Institute for Biological Studies, La Jolla, California, USA. [2]MRC Centre for Inflammation Research, University of Edinburgh, Edinburgh, UK. [3]Immunobiology and Microbial Pathogenesis Laboratory, Salk Institute for Biological Studies, La Jolla, California, USA. Correspondence should be addressed to G.L. (lemke@salk.edu).

Received 21 May; accepted 5 August; published online 7 September 2014; doi:10.1038/ni.2986

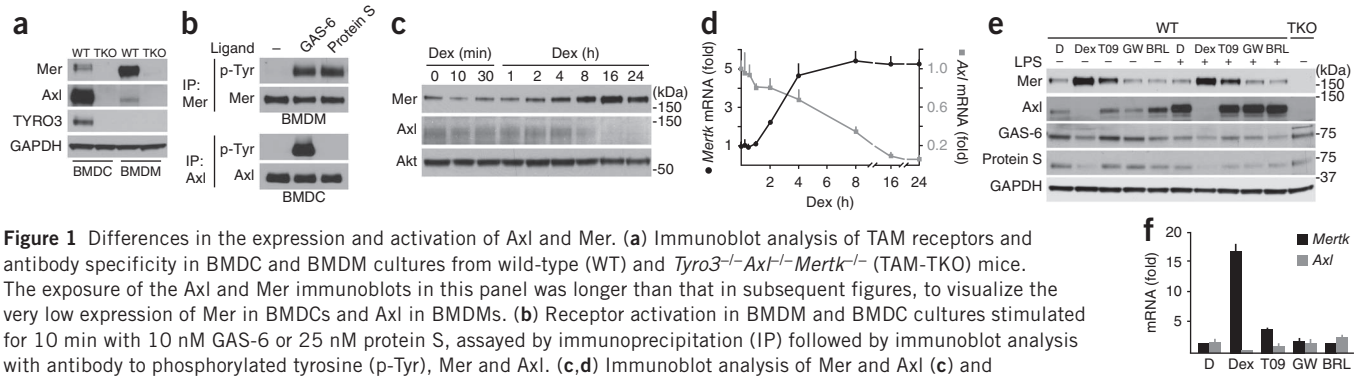

Figure 1 Differences in the expression and activation of Axl and Mer. (**a**) Immunoblot analysis of TAM receptors and antibody specificity in BMDC and BMDM cultures from wild-type (WT) and *Tyro3*$^{-/-}$*Axl*$^{-/-}$*Mertk*$^{-/-}$ (TAM-TKO) mice. The exposure of the Axl and Mer immunoblots in this panel was longer than that in subsequent figures, to visualize the very low expression of Mer in BMDCs and Axl in BMDMs. (**b**) Receptor activation in BMDM and BMDC cultures stimulated for 10 min with 10 nM GAS-6 or 25 nM protein S, assayed by immunoprecipitation (IP) followed by immunoblot analysis with antibody to phosphorylated tyrosine (p-Tyr), Mer and Axl. (**c**,**d**) Immunoblot analysis of Mer and Axl (**c**) and quantitative RT-PCR analysis of *Mertk* and *Axl* mRNA (**d**) in BMDM cultures upon stimulation with 0.1 μM Dex; mRNA results (**d**) were normalized to those of *Hprt* mRNA (encoding hypoxanthine guanine phosphoribosyl transferase) and are presented relative to those of untreated cells. Right margin (**c**), molecular size, in kilodaltons (kDa). (**e**,**f**) Immunoblot analysis of Mer and Axl (**e**) and quantitative RT-PCR analysis of *Mertk* and *Axl* mRNA (**f**) in BMDM cultures stimulated for 24 h with dimethylsulfoxide (D) as a control or with the nuclear receptor agonists Dex (1 μM), T0901317 (T09) (1 μM), GW501516 (GW) (0.2 μM) or BRL49653 (BRL) (1 μM), with (+) or without (–) the addition of LPS (30 ng/ml) 8 h before lysis; mRNA results (**f**) normalized and presented as in **d**. Data are representative of two (**a**,**c**,**e**) or three (**b**) independent experiments or are from two independent experiments with technical duplicates (**d**,**f**; mean and s.d.).

DCs. For example, in the spleen, CD68$^+$ tingible body macrophages were mainly Mer$^+$ (ref. 17), whereas CD11c$^+$ white pulp DCs were mostly Axl$^+$ (ref. 18) (**Supplementary Fig. 1**). In contrast, we found that CD11c$^+$CD11b$^-$MHCII$^-$ cells in the lung had abundant expression of Axl but low expression of Mer (**Supplementary Fig. 1**). We also observed some populations, such as red pulp macrophages in the spleen and Kupffer cells in the liver, in which Axl and Mer were coexpressed (**Supplementary Fig. 1**). Finally, we detected divergent expression of Mer and Axl in BMDM cultures: individual BMDM cells expressed either Mer or Axl, but not both (**Supplementary Fig. 2a**, top row).

Induction of Mer expression by tolerogenic stimuli

The differences in the expression of Axl and Mer in macrophages and DCs was matched by reciprocal responses to tolerogenic stimuli. The immunosuppressive glucocorticoid dexamethasone (Dex) has been shown to upregulate expression of Mer in human monocyte-derived macrophages[19], and we found that this was also true for mouse BMDMs (**Fig. 1c** and **Supplementary Fig. 2b**). Over a 24-hour time course, Dex mediated upregulation of the expression of Mer protein and the corresponding *Mertk* mRNA, and downregulation of the expression of Axl protein and *Axl* mRNA (**Fig. 1c**,**d** and **Supplementary Fig. 2c**). As other nuclear hormones have been reported to upregulate macrophage expression of Mer[20,21], we tested three other agonists of nuclear hormone receptors: the LXR agonist T0901317, the PPAR-δ agonist GW501516 and the PPAR-γ agonist BRL49653. Of these, only the LXR agonist potentiated Mer expression (**Fig. 1e**). Although lipopolysaccharide (LPS) was a potent inducer of Axl expression in BMDMs, coincubation with Dex suppressed this effect (**Fig. 1e**). Dex-mediated induction of Mer expression and suppression of Axl expression occurred at the mRNA level (**Fig. 1d**,**f**). In addition to Dex, the related corticosteroids hydrocortisone and aldosterone also induced Mer expression in BMDMs (**Supplementary Fig. 3**).

Glucocorticoid immunosuppression is marked by changes in macrophage gene expression and the inhibition of mitogen-activated protein kinase signaling pathways[22]. As we found that upregulation of *Mertk* in response to Dex was faster than the induction of canonical Dex targets such as *Fpr1* or *Mrc1* (**Supplementary Fig. 4a**), we investigated whether any of these canonical Dex effects might depend on upregulation of Mer expression or downregulation of Axl expression. We found that Dex-mediated inhibition of LPS-induced tumor-necrosis factor (TNF) (**Supplementary Fig. 4b**), Dex-mediated changes in gene expression (**Supplementary Fig. 4c**) and Dex inhibition of signaling via mitogen-activated protein kinases and the kinase Akt (**Supplementary Fig. 4d**) were all independent of Axl and Mer.

Induction of Axl expression by inflammatory stimuli

The polarization of macrophages into a 'classically activated' M1 phenotype is stimulated by Toll-like receptor (TLR) ligands and interferon-γ (IFN-γ); their polarization into an 'alternatively activated' M2 phenotype is stimulated by interleukin 4 (IL-4) and IL-13; and their polarization into a 'regulatory-tolerogenic' phenotype is stimulated by anti-inflammatory agents[23]. We found that the expression of Axl by BMDMs was potently stimulated by inflammatory mediators of classical M1 activation, which in general had modest inhibitory effects on Mer expression. LPS, for example, elevated *Axl* mRNA abundance over a time course that closely followed the induction of *Nos2* mRNA, which encodes inducible nitric oxide synthetase (**Fig. 2a**). (There was almost no basal expression of *Nos2* mRNA before stimulation (**Fig. 2a**).) Over the same time course, expression of *Gas6* mRNA and *Pros1* mRNA, which encode GAS-6 and protein S, respectively, was modestly reduced (**Fig. 2a**), as published before[24].

We surveyed a panel of pattern-recognition receptor ligands for their ability to regulate Axl and Mer expression in BMDMs (**Fig. 2b**). Axl expression was elevated by many of these inflammatory mediators, the most potent of which were ligands for TLR3, TLR4 and RIG-I, such as LPS and poly(I:C) (**Fig. 2b,c**). TNF and IFN-α also elevated Axl expression (**Fig. 2c**). TLR ligands induce Axl expression in DCs via type I interferons, as DCs deficient in interferon receptors fail to upregulate Axl in response to poly(I:C)[5]. Accordingly, we found that the upregulation of Axl expression by IFN-α in BMDMs was slightly faster than its upregulation by poly(I:C) (**Supplementary Fig. 5**). IFN-γ potently induced the expression of both Axl and Mer (**Fig. 2c**). However, individual BMDMs in IFN-γ-treated cultures were again either Mer$^+$ or Axl$^+$; only a small minority of these cells coexpressed both receptors (**Supplementary Fig. 2a**, bottom row).

Although the results reported above were consistent with Axl's being a marker of M1 activation, we found that IL-4 also elevated Axl expression and inhibited Mer expression in BMDMs (**Fig. 2d**). As expected, these reciprocal changes in receptor expression were paralleled by reciprocal changes in the autophosphorylation of Mer and

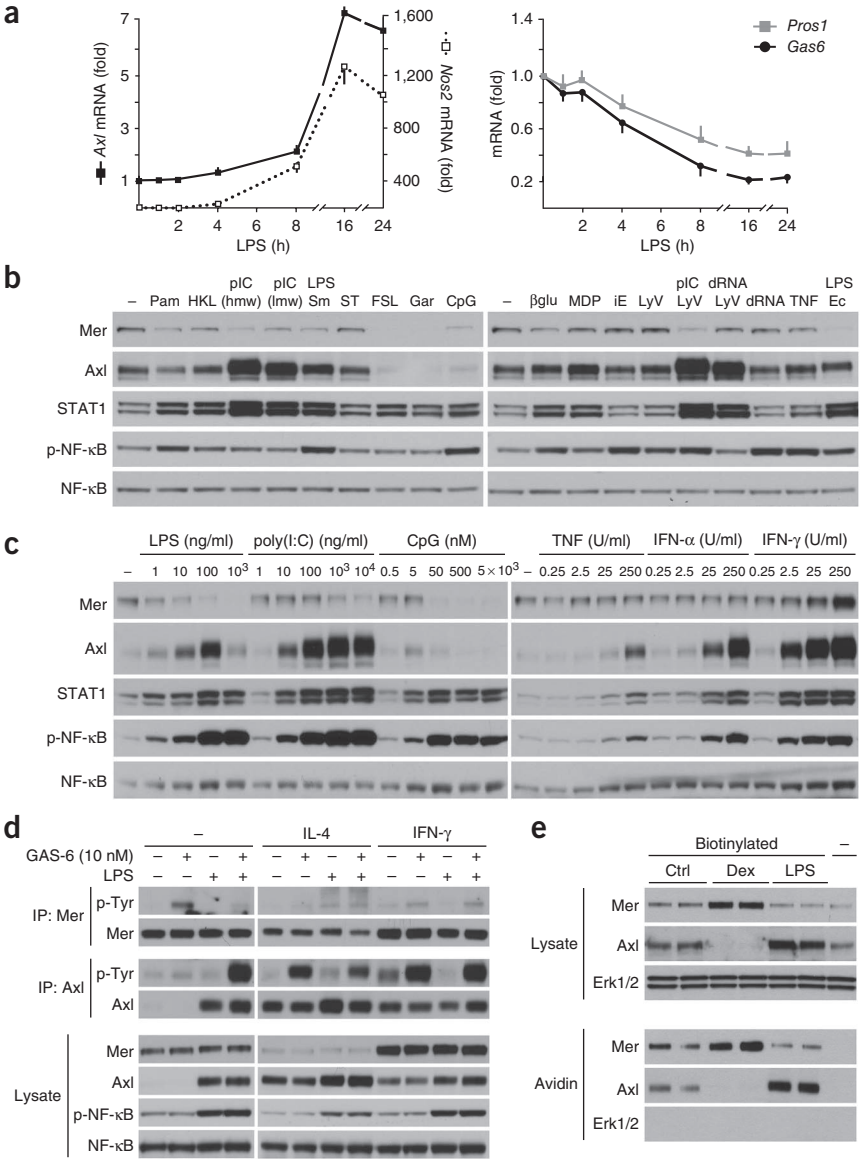

Figure 2 The expression of Axl and Mer in inflammatory macrophages. (**a**) Quantitative RT-PCR analysis of *Axl*, *Nos2*, *Gas6* and *Pros1* mRNA in BMDM cultures treated with 100 ng/ml of LPS (results normalized and presented as in **Fig. 1d**). (**b**) Immunoblot analysis of Mer and Axl in lysates of BMDMs stimulated for 18 h as follows (left to right lanes): Pam_3CSK_4 (TLR1 and TLR2 ligand), 100 ng/ml; HKLM (TLR2 ligand), 2×10^7 cells per ml; poly(I:C) (pIC; TLR3 ligand) of high molecular weight (hmw) or low molecular weight (lmw), 1 μg/ml; LPS from *Salmonella minnesota* (TLR4 ligand), 100 ng/ml; ST-FLA (TLR5 ligand), 100 ng/ml; FSL-1 (TLR6 and TLR2 ligand), 100 ng/ml; gardiquimod (TLR7 ligand), 1 μg/ml; CpG (ODN1826; TLR9 ligand), 0.5 μM; β-glucan (dectin ligand), 1 μM; MDP (Nod2 ligand), 10 μg/ml; iE-DAP (Nod1 ligand), 10 μg/ml; Lyo vector (control); triphosphate double-stranded RNA–Lyo vector (RIG-I ligand), 0.5 μg/ml; poly(I:C)–Lyo vector (RIG-I and Mda5 ligand), 1 μg/ml; triphosphate double-stranded RNA (control), 0.5 μg/ml; TNF, 25 U/ml; or LPS from *Escherichia coli* (TLR4 ligand), 100 ng/ml. STAT1 and phosphorylated NF-κB (p-NF-κB) serve as activation markers; total NF-κB serves as lysate loading control (**b**–**d**). (**c**) Immunoblot analysis of Mer and Axl BMDMs stimulated for 18 h with various concentrations (above lanes) of LPS, poly(I:C), CpG, TNF, IFN-α or IFN-γ. (**d**) Abundance and activation of receptors in BMDM cultures treated for 18 h with IL-4 (4 ng/ml) or IFN-γ (25 U/ml), with or without LPS (100 ng/ml), and then stimulated for 10 min with GAS-6 (10 nM), assayed by immunoprecipitation and immunoblot analysis. (**e**) Avidin-precipitation analysis of Axl and Mer on the surface of BMDM cultures treated for 18 h with Dex (0.1 μM) or LPS (100 ng/ml) and biotinylated before lysis. The kinase Erk1/2 serves as an intracellular control. Data are from two independent experiments with technical duplicates (**a**; mean ± s.d.) or are representative of two (**b**–**d**) or three (**e**) independent experiments.

Axl in response to recombinant GAS-6 (**Fig. 2d**). Through analysis with surface biotinylation, we verified that Dex-mediated stimulation of Mer and LPS-mediated stimulation of Axl were both associated with increased expression of these receptors on the cell surface (**Fig. 2e**). Together these observations indicated that Axl and Mer had divergent profiles of expression and regulation in inflammatory settings versus tolerogenic settings. In general, the induction of Mer expression was accompanied by the inhibition of Axl, and vice versa.

TAM specialization during phagocytosis

Genetic analyses have shown that Mer is required for the phagocytosis of apoptotic cells in various tissues[2,6,7,9,25], but a possible role for Axl in this process has been less well studied[18,26]. We first examined the mobilization of Axl and Mer to the surface of BMDMs in contact with apoptotic thymocytes. We labeled the apoptotic cells with a cytoplasmic dye (CellTracker Orange) and incubated them with BMDMs for 30 min. In the absence of a TAM ligand, neither Axl nor Mer was localized to the site at which the BMDM associated with the apoptotic cell (**Fig. 3a**,**b**, left). However, upon the addition of either GAS-6 or protein S to Mer^+ BMDMs or of GAS-6 (but not protein S) to Axl^+ BMDMs, we observed substantial relocalization of Mer and Axl to the membrane surrounding entrapped apoptotic cells (**Fig. 3a–c**). Poly(I:C)-treated Axl^+ BMDMs formed a readily apparent phagocytic cup during the engulfment of apoptotic cells, as visualized by scanning electron microscopy (**Fig. 3d**).

To assess quantitatively the ability of Axl to mediate the phagocytosis of apoptotic cells, we analyzed wild-type, $Axl^{-/-}$ and $Mertk^{-/-}$ macrophages by a flow cytometry–based phagocytosis assay that exploits pHrodo[27], a pH-sensitive fluorescent dye (**Supplementary Fig. 6**). We used untreated BMDM cultures and cultures treated with Dex, poly(I:C) or IFN-γ for these experiments. We found that untreated (Mer-expressing) BMDMs had a modest phagocytic index that was increased by either GAS-6 or protein S, and that the phagocytosis of apoptotic cells was Mer dependent and Axl independent (**Fig. 3e**). Stimulation of phagocytosis was significantly enhanced in Dex-treated cells (**Fig. 3f**). In contrast, phagocytosis by poly(I:C)-treated, Axl-expressing BMDMs was stimulated only by GAS-6, and this stimulation was entirely Axl dependent (**Fig. 3g**). IFN-γ-treated BMDM cultures contained cells with high expression of either Axl or Mer (**Supplementary Fig. 2a**, bottom). Phagocytic activity in these

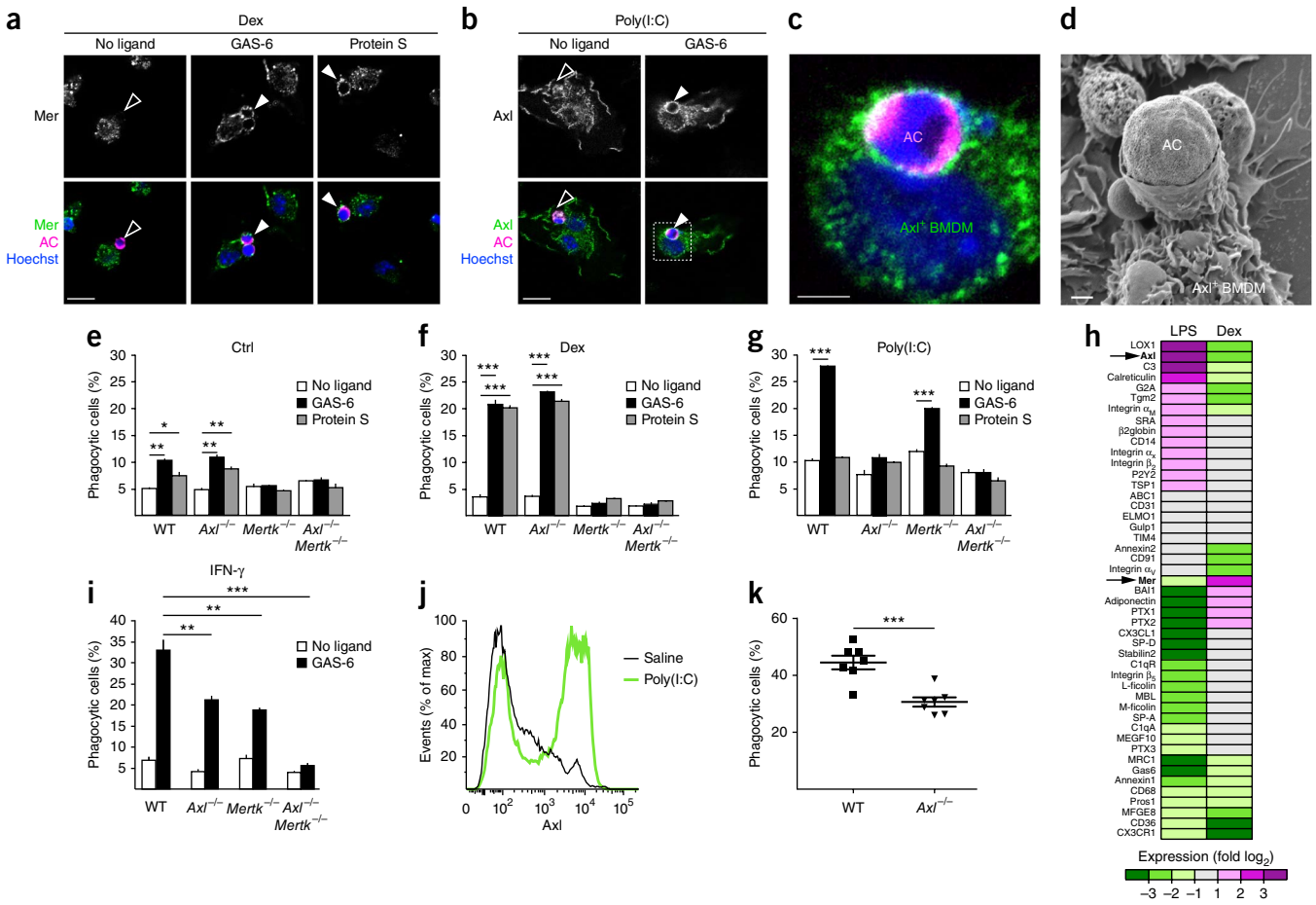

Figure 3 Axl is a phagocytic receptor in activated macrophages. (**a**–**c**) Immunostaining of Mer and Axl in cells from BMDM cultures treated for 24 h with 0.1 μM Dex (**a**) or 10 μg/ml of poly(I:C) (**b**,**c**) and then incubated for 30 min with apoptotic cells (AC) stained with CellTracker Orange in the presence or absence of TAM ligands (GAS-6 or protein S); **c** is an enlargement of the area outlined (dashed line) in **b**. Open arrowheads, non-engulfed apoptotic cells attached to TAM-negative membrane; filled arrowheads, engulfed apoptotic cells surrounded by TAM-positive membrane. Scale bars, 20 μm (**a**,**b**) or 5 μm (**c**). (**d**) Scanning electron microscopy of poly(I:C)-treated BMDM cells (as in **b**,**c**). Scale bar, 1 μm. (**e**–**g**,**i**) Phagocytosis in wild-type, *Axl*$^{-/-}$, *Mertk*$^{-/-}$ and *Axl*$^{-/-}$*Mertk*$^{-/-}$ BMDM cultures left untreated (Ctrl; **e**) or treated for 24 h with 0.1 μM Dex (**f**), 10 μg/ml of poly(I:C) (**g**) or 250 U/ml of IFN-γ (**i**), then incubated for 1 h with pHrodo-labeled apoptotic cells with or without TAM ligands and analyzed by flow cytometry. $^{*}P < 0.05$, $^{**}P < 0.01$ and $^{***}P < 0.001$ (unpaired two-tailed *t*-test). (**h**) Quantitative RT-PCR analysis of genes encoding various proteins (left margin) in BMDMs left untreated or treated for 24 h with 0.1 μM Dex or 100 ng/ml of LPS; results ($\log_2$) were normalized to that of mRNA encoding cyclophilin A and are presented relative to those of untreated cells. $P < 0.05$ (two-tailed *t*-test). (**j**) Axl expression on CD11b^{+} peritoneal macrophages collected from wild-type mice by peritoneal lavage 16 h after intraperitoneal injection of saline or 100 μg poly(I:C), measured by flow cytometry. (**k**) Phagocytosis by CD11b^{+} macrophages from wild-type mice ($n = 7$) or *Axl*$^{-/-}$ mice ($n = 7$) given intraperitoneal injection of 100 μg poly(I:C) for 16 h, followed by injection of pHrodo-labeled apoptotic cells for 1 h; macrophages were collected by peritoneal lavage and quantified by flow cytometry. Each symbol represents an individual mouse; small horizontal lines indicate the mean (±s.e.m.). $P = 0.0004$ (two-tailed *t*-test). Data are representative of two independent experiments with ten images per condition (**a**–**d**), two independent experiments with three mice per condition (**j**), two independent experiments with duplicate cultures for each genotype and each condition (**e**–**g**,**i**; mean and s.d.) or three independent experiments (**h**) or are pooled from two independent experiments (**k**).

cultures also was potentiated by GAS-6, and this potentiation was completely absent only in *Axl*$^{-/-}$*Mertk*$^{-/-}$ cultures (**Fig. 3i**). Together these results demonstrated that both Axl and Mer functioned as phagocytic receptors *in vitro*, but that they acted in different settings and relied on different ligands.

Basal phagocytosis was decreased in Dex-treated cells and elevated in poly(I:C)-treated cells, and neither of these effects was TAM dependent (**Fig. 3f,g**). We therefore measured changes in mRNAs encoding other known factors that mediate the recognition and engulfment of apoptotic cells in response to both pro- and anti-inflammatory stimuli. We found that many of these were coregulated with either Axl or Mer. For example, mRNA encoding the C-type lectin LOX-1 (ref. 28) was coregulated with Axl (**Fig. 3h**), whereas mRNA encoding the PtdSer receptor BAI1 (ref. 29) was coregulated with Mer (**Fig. 3h**). These results indicated that activated macrophage populations and tolerogenic macrophage populations used distinct cohorts of phagocytic mediators to recognize and engulf apoptotic cells.

To assess the ability of Axl to mediate the phagocytosis of apoptotic cells by macrophages *in vivo*, we intraperitoneally administered pHrodo-labeled apoptotic cells 16 h after injection of poly(I:C) and allowed 1 h for phagocytosis before isolating peritoneal macrophages. CD11b^{+} peritoneal macrophages had high expression of Axl in response to injection of poly(I:C) (**Fig. 3j**). We found that poly(I:C)-treated *Axl*$^{-/-}$macrophages phagocytized apoptotic cells less efficiently than their wild-type counterparts did (**Fig. 3k**).

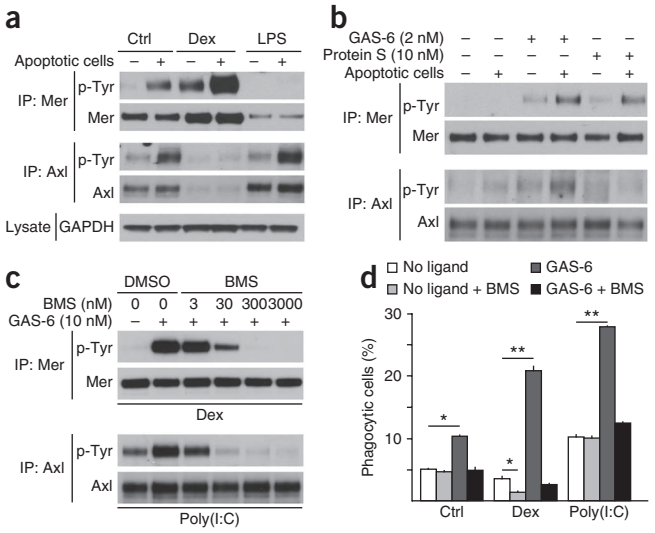

Figure 4 Axl and Mer kinase activity is necessary for the phagocytosis of apoptotic cells. (**a**) Receptor activation in BMDM cultures left unstimulated (Ctrl) or stimulated for 18 h with 0.1 μM Dex or 100 ng/ml of LPS and then incubated for 30 min with (+) or without (–) apoptotic cells at a ratio of 1:10, assayed by immunoprecipitation and immunoblot analysis. (**b**) Receptor activation in BMDM cultures 'starved' for 18 h, washed, and then stimulated for 10 min with 2 nM GAS-6 or 10 nM protein S with or without apoptotic cells, assayed as in **a**. (**c**) Receptor activation in BMDMs cultured for 18 h with 0.1 μM Dex or 10 μg/ml poly(I:C), pretreated for 15 min with BMS-777607 and then stimulated for 10 min with 10 nM GAS-6, assayed as in **a**. (**d**) Phagocytosis in BMDM cultures left untreated (Ctrl) or treated for 24 h with 0.1 μM Dex or 10 μg/ml of poly(I:C), then incubated for 1 h with pHrodo-labeled apoptotic cells and with or without 10 nM GAS-6 and 300 nM BMS-777607, quantified by flow cytometry. $*P < 0.01$ and $**P < 0.001$ (unpaired two-tailed *t*-test). Data are representative of two independent experiments (**a**–**c**) or are from two independent experiments with duplicate cultures for each condition (**d**; mean and s.d.).

We also assayed the potential role of TYRO3 in the phagocytosis of apoptotic cells by BMDCs. BMDCs had minimal expression of TYRO3, and this expression was further downregulated by proinflammatory stimuli. The regulation and activation of Axl and Mer in BMDCs paralleled that observed for BMDMs (**Supplementary Fig. 7a**,**b**). Through the use of BMDCs from *Tyro3*$^{-/-}$ mice, we found that TYRO3 was not required for Dex-induced Mer-dependent phagocytosis of apoptotic cells or for poly(I:C)-induced Axl-dependent phagocytosis of apoptotic cells (**Supplementary Fig. 7c**,**d**). The minimal TYRO3 expressed by BMDCs therefore did not have a substantial role in the phagocytosis of apoptotic cells.

TAM activity during phagocytosis

We assessed the ability of apoptotic cells, in concert with TAM ligands, to modulate TAM receptor kinase activity in BMDMs. GAS-6 and protein S were produced by BMDMs (**Fig. 1e**), and culture medium supplemented with 10% serum contained ~30 nM protein S. The addition of apoptotic cells to BMDMs for 30 min potentiated autophosphorylation of Axl and, to a greater extent, that of Mer (**Fig. 4a**). Dex-treated cells exhibited more Mer kinase activity, which was further elevated by the addition of apoptotic cells, whereas no Axl activity was detectable (**Fig. 4a**). Conversely, LPS-treated BMDMs exhibited enhanced autophosphorylation of Axl, but no activation of Mer, upon exposure to apoptotic cells (**Fig. 4a**).

To control ligand concentrations in this assay, we cultured untreated BMDMs overnight in serum-free medium and washed the cells extensively before the assay. We then added low concentrations of purified ligands, 2 nM GAS-6 or 10 nM protein S, with or without the addition of apoptotic cells, and assayed the autophosphorylation of Mer and Axl. Without added GAS-6 or protein S, the presence of apoptotic cells alone had no effect on the basal kinase activity of either Mer or Axl (**Fig. 4b**). The addition of GAS-6 increased the phosphorylation of Mer and, to lesser extent, that of Axl, consistent with the much higher expression of Mer than of Axl in these cultures (**Fig. 4b**). The activation of Mer and Axl by GAS-6 was substantially enhanced by the inclusion of apoptotic cells (**Fig. 4b**). Protein S likewise stimulated the autophosphorylation of Mer, which was also enhanced by the inclusion of apoptotic cells, but protein S had no such effect on Axl (**Fig. 4b**).

To determine whether tyrosine kinase activity of the TAM receptors is required for the phagocytosis of apoptotic cells, we used BMS-777607, a small-molecule inhibitor of the Met, Ron and TAM RTKs[30]. This compound efficiently inhibits GAS-6-driven activation of both Mer and Axl in BMDCs[10]. We observed the same degree of the inhibition of TAM receptors in BMDMs (**Fig. 4c**). When we added BMS-777607 to BMDMs grown under basal conditions or in the presence of Dex or poly(I:C), we found that BMS-777607 blocked phagocytosis in all settings (**Fig. 4d**). Thus, Axl and Mer tyrosine kinase activities were both induced and required for TAM-dependent apoptotic cell phagocytosis.

Axl-dependent GAS-6 expression *in vivo*

We observed that the maintenance of GAS-6 in many tissues was entirely dependent on simultaneous expression of Axl. Although we readily detected GAS-6 by immunohistochemistry in sections of spleen, small intestine, liver and lung from wild-type mice, its expression was lost in those tissues from *Axl*$^{-/-}$ mice (**Fig. 5a**). This effect was specific to Axl, as the presence of GAS-6 was unaltered in those tissues in *Mertk*$^{-/-}$ mice (**Fig. 5a**) and *Tyro3*$^{-/-}$ mice (data not shown). Immunoblot analysis of GAS-6 in splenic lysates confirmed the results obtained by *in vivo* immunostaining (**Fig. 5b**). Consistent with the hypothesis that most or all splenic GAS-6 is normally bound to Axl, we found that the basal phosphorylation of Axl was slightly higher in wild-type spleens than in *Gas6*$^{-/-}$ splenic lysates (**Fig. 5c**), but this basal Axl activation was still far below that observed upon the addition of GAS-6 *in vitro* (**Fig. 1b**) or upon the addition of activating antibody to Axl *in vivo* (reported below).

When we costained sections of wild-type splenic red pulp with antibody to Axl (anti-Axl) and anti-GAS-6, we observed perfect colocalization (**Fig. 5d**). Similarly, when we stained poly(I:C)-treated BMDM cultures, we found that BMDMs displaying surface Axl were always the same cells that displayed surface GAS-6, and vice versa (**Fig. 5e**). Specific steady-state binding of GAS-6 to Axl may have accounted for the higher basal activation of Axl than that of Mer (**Fig. 4a**,**c**). The absence of GAS-6 in *Axl*$^{-/-}$ spleens (**Fig. 5a**) was not due to an inability of *Axl*$^{-/-}$ splenic macrophages to express the *Gas6* gene, as we saw no difference in the *Gas6* mRNA in *Axl*$^{-/-}$ spleens and wild-type spleens (**Fig. 5f**). The translation of GAS-6 protein also occurred normally in *Tyro3*$^{-/-}$*Axl*$^{-/-}$*Mertk*$^{-/-}$ BMDMs in culture (**Fig. 1e**). Finally, the 'missing GAS-6' of *Axl*$^{-/-}$ tissues did not accumulate in the circulation, as the low concentration of GAS-6 normally present in serum was unchanged in *Axl*$^{-/-}$ mice (**Fig. 5g**). Together these data indicated that maintenance of a GAS-6 protein reservoir in many tissues was dependent on the surface expression of Axl and that in these tissues GAS-6 was normally prebound to Axl. We know of no equivalent dependence for other RTKs and their ligands.

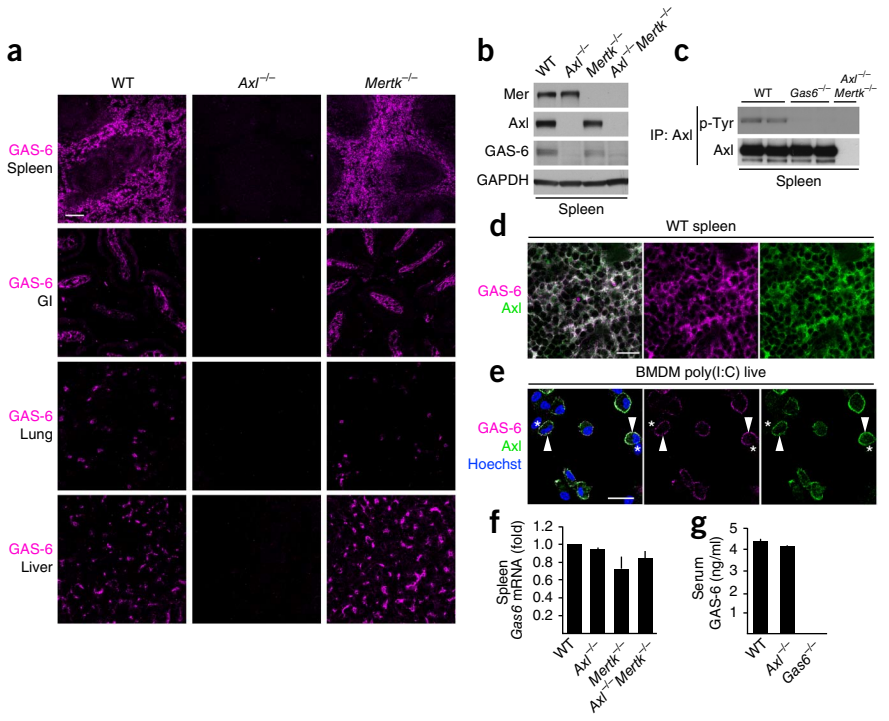

Figure 5 GAS-6 is bound to Axl *in vivo* and *in vitro*. (**a**) Immunohistochemistry of GAS-6 in spleen, duodenum (GI), lung and liver sections from wild-type, *Axl*$^{-/-}$ and *Mertk*$^{-/-}$ mice ($n = 3$ per genotype). Scale bar, 100 µm. (**b**) Immunoblot analysis of Axl, Mer and GAS-6 in spleen extracts from wild-type, *Axl*$^{-/-}$, *Mertk*$^{-/-}$ and *Axl*$^{-/-}$*Mertk*$^{-/-}$ mice. (**c**) Basal activation of Axl in wild-type, *Gas6*$^{-/-}$ and *Axl*$^{-/-}$*Mertk*$^{-/-}$ mouse spleens, assayed by immunoprecipitation and immunoblot analysis (each lane is from an independent mouse). (**d**) Colocalization of Axl and GAS-6 in spleen red pulp from wild-type mice ($n = 3$). Scale bar, 20 µm. Analysis of sections from *Axl*$^{-/-}$ and *Gas6*$^{-/-}$ mice confirmed antibody specificity (data not shown). (**e**) Colocalization of Axl and GAS-6 on the surface of poly(I:C)-treated live BMDMs: arrowheads, cells costained with anti-Axl and anti–GAS-6; asterisks, cells negative for both Axl and GAS-6. Scale bar, 20 µm. Analysis of cells from *Axl*$^{-/-}$ and *Gas6*$^{-/-}$ mice confirmed antibody specificity (data not shown). (**f**) Quantitative RT-PCR analysis of *Gas6* mRNA in spleens from wild-type, *Axl*$^{-/-}$, *Mertk*$^{-/-}$ and *Axl*$^{-/-}$*Mertk*$^{-/-}$ mice ($n = 2$ per genotype); results were normalized to that of mRNA encoding actin and are presented relative to those of wild-type mice. (**g**) Enzyme-linked immunosorbent assay of GAS-6 in serum from wild-type, *Axl*$^{-/-}$ and *Gas6*$^{-/-}$ mice ($n = 3$ per genotype). Data are representative of three experiments (**a**,**d**) or two independent experiments (**b**,**c**,**e**) or are from one experiment with samples pooled from two (**f**) or three (**g**) mice per genotype (**f**,**g**; mean and s.d.).

Antibody-mediated TAM activation

RTKs are activated by ligand-driven dimerization and multimerization of receptor subunit monomers[31]. Thus, antibodies generated against RTK ectodomains often act as ligand-independent RTK activators through their ability to drive receptor dimerization[32,33]. Although cross-activation of Mer has been achieved with a combination of primary and secondary antibodies[34], directly activating antibodies to the TAM receptors have not yet been reported. We found that affinity-purified, polyclonal anti-Axl (AF854; R&D Systems), anti-Mer (AF591; R&D Systems) and anti-TYRO3 (AF759; R&D Systems) activated their respective receptors (**Fig. 6a** and data not shown). In contrast to GAS-6, which activated all three TAM receptors, anti-Mer and anti-Axl displayed absolute receptor specificity (**Fig. 6b**).

We assessed the utility of these antibodies as TAM activators *in vivo*. We first injected anti-Axl intravenously and monitored activation and expression of Axl and Mer in the spleen. We found that splenic Axl was activated within 15 min after injection and that its activity returned to baseline by 24 h (**Fig. 6c**). Mer was not activated by anti-Axl, and control immunoglobulin G (IgG) had no effect on the activation or expression of Axl (**Fig. 6c**). As noted before[35,36], we found that strong activation of Axl led to the rapid cleavage of the Axl ectodomain from the cell surface, a consequent loss of steady-state Axl, and the appearance of soluble Axl ectodomain (**Fig. 6c**).

We next assessed whether varying doses of the antibodies could activate their receptors in liver, lung and spleen. We detected dose-dependent activation of Axl in spleen and lung, again associated with splenic cleavage of Axl, which was especially notable at the highest antibody dose (**Fig. 6d**). In the liver, cleavage of Axl was so robust that we were unable to detect any remaining Axl protein 1 h after injection of either 50 µg or 10 µg of the antibody (**Fig. 6d**). We also observed dose-dependent activation of Mer in these tissues at 1 h after injection of anti-Mer (**Fig. 6e**). The activation of Mer was greatest in liver and lung and, in contrast to results obtained for Axl, it was not associated with cleavage or loss of Mer protein (**Fig. 6e**). These results indicated that activating antibodies functioned as specific tools for the activation of individual TAM receptors.

TAM activation alone is insufficient for phagocytosis

The TAM-activating antibodies allowed us to assess whether TAM activation in the absence of ligand could promote phagocytosis. We found that the addition of either activating antibody to Axl or activating antibody to Mer alone, in the absence of added GAS-6, had no stimulatory effect on the phagocytosis of apoptotic cells (**Fig. 6f**,**g**). Moreover, the addition of these receptor-activating antibodies in the presence of GAS-6 actually inhibited the GAS-6-stimulated phagocytosis of apoptotic cells (**Fig. 6f**,**g**). This inhibition could have resulted from competition between the antibody and GAS-6 for receptor binding or, for anti-Axl, antibody-induced cleavage of Axl. Thus, TAM activation was necessary for the phagocytosis of apoptotic cells by macrophages (**Fig. 4d**), but activation in the absence of a tripartite receptor–ligand–apoptotic cell (PtdSer) bridging interaction[8] was not sufficient for phagocytosis.

Axl activation inhibits inflammatory responses *in vivo*

As the activation of Axl in DCs inhibits the production and signaling of type I interferons[5], we hypothesized that treatment with the activating antibody to Axl, even though it did not promote phagocytosis, might be anti-inflammatory *in vivo*. To test this possibility, we gave mice intraperitoneal injection of LPS (or saline as a control) together with either the activating antibody to Axl or control IgG, then measured mRNAs encoding type I interferons in the spleen 2 h after injection. We observed marked suppression of *Ifnb1* mRNA and *Ifna4* mRNA in mice given injection of anti-Axl but not in those given injection of control IgG (**Fig. 6h**,**i**). These results suggested that activating antibodies to Axl might be a viable approach to TAM-specific immunosuppressive therapeutics. Overall, our results

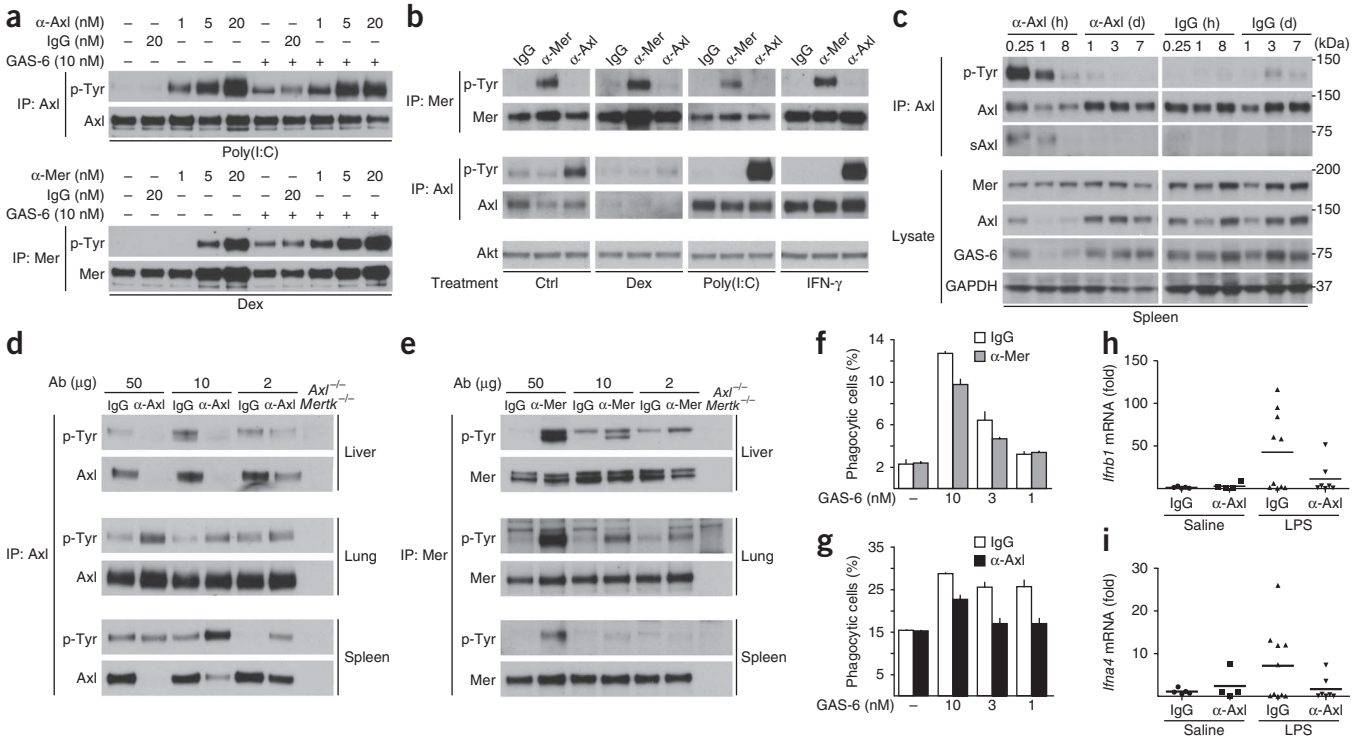

Figure 6 Axl- and Mer-activating antibodies. (**a**) Receptor activation in BMDM cultures pretreated for 18 h with 0.1 μM Dex or 10 μg/ml of poly(I:C), then stimulated for 20 min with control antibody (IgG) or activating antibody to Axl (α-Axl) or Mer (α-Mer), with or without addition of 10 nM GAS-6 for the final 10 min, assayed by immunoprecipitation and immunoblot analysis. (**b**) Receptor activation in BMDM cultures pretreated for 18 h with 0.1 μM Dex, 10 μg/ml of poly(I:C) or 250 U/ml of IFN-γ, then stimulated for 10 min with 10 nM of an activating antibody, assayed as in **a**. (**c**) Activation of Axl in spleens collected from mice injected intravenously with 10 μg of activating antibody to Axl or control IgG, assayed as in **a**; below, immunoblot analysis of total spleen lysates. sAxl, soluble Axl ectodomain. (**d**,**e**) Dose-dependent receptor activation in livers, lungs and spleen of mice given intravenous injection for 1 h of anti-Axl (**d**), anti-Mer (**e**) or control IgG. Ab, antibody. (**f**,**g**) Phagocytosis in BMDM cultures pretreated for 24 h with 0.1 μM Dex (**f**) or 10 μg/ml of poly(I:C) (**g**) and then treated with 10 nM activating antibody to Mer (**f**) or Axl (**g**) and increasing concentrations (horizontal axis) of GAS-6 during phagocytosis. (**h**,**i**) Quantitative RT-PCR analysis of *Ifnb1* (**h**) and *Ifna4* (**i**) in spleen from wild-type mice given intraperitoneal injection of saline or 10 μg LPS together with 10 μg of control IgG or activating antibody to Axl; results were normalized to that of mRNA encoding cyclophilin A and are presented relative to those of mice given of saline and IgG. Each symbol represents an individual mouse ($n = 5$ (saline and IgG), $n = 4$ (saline and anti-Axl), $n = 10$ (LPS and IgG) or $n = 7$ (LPS and anti-Axl)); short horizontal lines indicate the mean. Data are representative of two independent experiments (**a**–**e**), are pooled from two independent experiments (**h**,**i**) or are from two independent experiments each with duplicate cultures for each condition (**f**,**g**; mean and s.d.).

demonstrated that Axl and Mer were operationally distinct receptors. Our data revealed a pronounced diversification of the expression, activity, function, ligand use and proteolytic processing of TAM receptors (**Supplementary Fig. 8**).

DISCUSSION

We found that Axl and Mer segregated into distinct niches of expression and function: Mer acted mainly in settings of steady-state and induced tolerance, whereas Axl was specialized to act in the feedback inhibition of inflammation. Inflammatory stimuli that elevated Axl expression tended to decrease Mer expression, and immunosuppressive stimuli that elevated Mer tended to decrease Axl expression. Axl expression was induced in both M1-polarized macrophages and M2-polarized macrophages, which suggested that it acts as a response receptor for nearly any inflammatory insult or tissue injury. Both Axl and Mer functioned as immunosuppressive phagocytic receptors, but they operated in inflammatory environments and tolerogenic environments, respectively.

When activated by ligand binding, Axl promotes the cleavage of its extracellular domain from the cell surface through the activation of proteases[35,36]. We found that such cleavage, which generated 'soluble Axl', also occurred when Axl was activated by crosslinking antibodies. Elevated soluble Axl in blood has been reported to mark multiple human disease and trauma states, including aortic aneurysm[37], lupus flares[38], pneumonia infection[39], preeclampsia[40], coronary bypass[41] and insulin resistance[42]. We suggest that cleavage of Axl and the generation of a soluble Axl–GAS-6 complex are triggered by the inflammation-induced exposure of PtdSer in these settings and may be a broadly useful diagnostic biomarker for inflammation in human disease.

Although Mer also acts to suppress inflammation[43,44], it does so in two settings that are very different from the inflammatory environment in which Axl operates. The first is in normal tissues that are subject to continuous cellular renewal throughout life, and in which billions of apoptotic cells are generated and cleared on a regular, often circadian, schedule[45,46]. The second is during enhanced immunotolerance induced by corticosteroids and LXR agonists[19,20]. We showed that the ability of these agents to stimulate phagocytosis of apoptotic cells was entirely dependent on their ability to upregulate macrophage expression of Mer.

Our data indicated that the pattern of Mer polarization in homeostatic settings and Axl polarization in inflammatory settings extended to various other phagocytic mediators. These results suggested that distinct subgroups of phagocytic receptors are specialized to

orchestrate the clearance of apoptotic cells in different environments. The cleavage of Axl upon its activation suggests that Axl may be required only for initial stages of the phagocytosis of apoptotic cells. This is in agreement with work suggesting that Axl is a tethering receptor for apoptotic cells and that it acts together with CD91 (LRP-1 ('low-density lipoprotein receptor–related protein 1')) for engulfment[18]. Consistent with that suggestion, we observed that CD91 was coregulated with Axl by Dex.

The segregation of Axl and Mer extended to their ligands. Unlike the other TAM receptors, Axl and GAS-6 were codependent: Axl uniquely depended on GAS-6 for its activation, and GAS-6 required Axl for its stable maintenance *in vivo*. The constitutive presence of an Axl–GAS-6 complex in tissues would suggest that exposure of PtdSer may be the actual trigger for Axl activation. Indeed, the low basal activity of Axl in complex with GAS-6 was substantially enhanced by exposure to PtdSer-rich membranes.

Their divergence notwithstanding, both Axl and Mer mediated the PtdSer-dependent phagocytosis of apoptotic cells, and our results have elucidated several features of the bridging model for this process[3,8]. In this model, GAS-6 or protein S binds concomitantly a TAM receptor on the phagocyte surface and PtdSer on the apoptotic cell. First, we showed that activation of TAM kinase activity was necessary for phagocytosis, which indicated that TAM receptors serve as more than passive docking sites for apoptotic cells on the surface of phagocytes. Second, we showed that activation of TAM kinases was not sufficient for the phagocytosis of apoptotic cells. And third, we observed rapid mobilization of the receptors to sites of apoptotic cell contact upon the addition of purified ligands. Thus, the interpolation of TAM ligand between the macrophage and its phagocytic target was obligatory.

TAM receptor divergence is relevant to human therapy. TAM inhibitors are in development for cancer therapies[13,47,48] and the treatment of infection with enveloped viruses[10], whereas TAM activators have been proposed as treatments for autoimmune indications[49,50]. The fact that Mer functions on a daily basis throughout decades of adult life suggests that its long-term inhibition in the course of a cancer therapy should be evaluated for side effects, including the development of impaired vision, diminished male fertility and autoimmune disease. Long-term inhibition of Axl may result in fewer adverse reactions. In several settings, antibody-based therapies may have the advantage of absolute receptor specificity. Notably, the finding that downregulation of Axl is brought about through ectodomain cleavage calls into question the utility of the activation of Axl as a vehicle for the delivery of cytotoxic drugs in Axl-overexpressing tumors. At the same time, the use of activating antibodies to Axl—for example, in the potential treatment of lupus or arthritis flares—should have the advantage of being self-limiting owing to this receptor cleavage. Our results indicate that such antibodies may also be effective in the control of inflammation subsequent to infection. These and related considerations suggest that modulation of TAM receptors is an especially promising approach to the treatment of human disease.

METHODS

Methods and any associated references are available in the online version of the paper.

Note: Any Supplementary Information and Source Data files are available in the online version of the paper.

ACKNOWLEDGMENTS

We thank M. Joens and J. Fitzpatrick for processing samples and acquiring scanning electron microscopic images; R. Evans (Salk Institute) for nuclear receptor agonists T0901317, GW501516 and BRL49653; J. Hash, P. Burrola and C. Mayer for technical support; and members of the Lemke laboratory and the Nomis Center for discussions. Supported by the US National Institutes of Health (R01 AI077058, R01 AI101400 and R01 NS085296 to G.L.), the Leona M. and Harry B. Helmsley Charitable Trust (2012-PG-MED002 to G.L.) the Nomis Foundation, the H.N. and Frances C. Berger Foundation, the Fritz B. Burns Foundation, the HKT Foundation, Françoise Gilot-Salk, the Human Frontiers Science Program (A.Z.), the Marie Curie Seventh Framework Programme (P.G.T.), the Leukemia and Lymphoma Society and the Nomis Foundation (E.D.L.).

AUTHOR CONTRIBUTIONS

A.Z. designed and performed the experiments; P.G.T. aided in the design and execution of *in vivo* experiments; E.D.L. prepared purified recombinant GAS-6; I.D. aided in the design of the flow-cytometry-based phagocytosis assay; G.L. contributed to the design of the experiments and wrote the manuscript.

COMPETING FINANCIAL INTERESTS

The authors declare competing financial interests: details are available in the online version of the paper.

1. Muñoz, L.E., Lauber, K., Schiller, M., Manfredi, A.A. & Herrmann, M. The role of defective clearance of apoptotic cells in systemic autoimmunity. *Nat. Rev. Rheumatol.* **6**, 280–289 (2010).
2. Lemke, G. Biology of the TAM receptors. *Cold Spring Harbor Perspectives* **5**, a009076 (2013).
3. Lemke, G. & Rothlin, C.V. Immunobiology of the TAM receptors. *Nat. Rev. Immunol.* **8**, 327–336 (2008).
4. Lu, Q. & Lemke, G. Homeostatic regulation of the immune system by receptor tyrosine kinases of the Tyro 3 family. *Science* **293**, 306–311 (2001).
5. Rothlin, C.V., Ghosh, S., Zuniga, E.I., Oldstone, M.B. & Lemke, G. TAM receptors are pleiotropic inhibitors of the innate immune response. *Cell* **131**, 1124–1136 (2007).
6. Burstyn-Cohen, T. *et al.* Genetic dissection of TAM receptor-ligand interaction in retinal pigment epithelial cell phagocytosis. *Neuron* **76**, 1123–1132 (2012).
7. Scott, R.S. *et al.* Phagocytosis and clearance of apoptotic cells is mediated by MER. *Nature* **411**, 207–211 (2001).
8. Lemke, G. & Burstyn-Cohen, T. TAM receptors and the clearance of apoptotic cells. *Ann. NY Acad. Sci.* **1209**, 23–29 (2010).
9. Lu, Q. *et al.* Tyro-3 family receptors are essential regulators of mammalian spermatogenesis. *Nature* **398**, 723–728 (1999).
10. Bhattacharyya, S. *et al.* Enveloped viruses disable innate immune responses in dendritic cells by direct activation of TAM receptors. *Cell Host Microbe* **14**, 136–147 (2013).
11. Meertens, L. *et al.* TIM and TAM receptors mediate dengue virus infection. *Cell Host Microbe* **12**, 544–557 (2012).
12. Paolino, M. *et al.* Essential role of E3 ubiquitin ligase activity in Cbl-b-regulated T cell functions. *J. Immunol.* **186**, 2138–2147 (2011).
13. Schlegel, J. *et al.* MERTK receptor tyrosine kinase is a therapeutic target in melanoma. *J. Clin. Invest.* **123**, 2257–2267 (2013).
14. Meyer, A.S., Miller, M.A., Gertler, F.B. & Lauffenburger, D.A. The receptor AXL diversifies EGFR signaling and limits the response to EGFR-targeted inhibitors in triple-negative breast cancer cells. *Sci. Signal.* **6**, ra66 (2013).
15. Carrera Silva, E.A. *et al.* T cell-derived protein S engages TAM receptor signaling in dendritic cells to control the magnitude of the immune response. *Immunity* **39**, 160–170 (2013).
16. Inaba, K. *et al.* Isolation of dendritic cells. *Curr. Protoc. Immunol.* **25**, 3.7 (2009).
17. Rahman, Z.S., Shao, W.H., Khan, T.N., Zhen, Y. & Cohen, P.L. Impaired apoptotic cell clearance in the germinal center by Mer-deficient tingible body macrophages leads to enhanced antibody-forming cell and germinal center responses. *J. Immunol.* **185**, 5859–5868 (2010).
18. Subramanian, M. *et al.* An AXL/LRP-1/RANBP9 complex mediates DC efferocytosis and antigen cross-presentation in vivo. *J. Clin. Invest.* **124**, 1296–308 (2014).
19. McColl, A. *et al.* Glucocorticoids induce protein S-dependent phagocytosis of apoptotic neutrophils by human macrophages. *J. Immunol.* **183**, 2167–2175 (2009).
20. A-Gonzalez, N. *et al.* Apoptotic cells promote their own clearance and immune tolerance through activation of the nuclear receptor LXR. *Immunity* **31**, 245–258 (2009).
21. Mukundan, L. *et al.* PPAR-delta senses and orchestrates clearance of apoptotic cells to promote tolerance. *Nat. Med.* **15**, 1266–1272 (2009).
22. Clark, A.R. Anti-inflammatory functions of glucocorticoid-induced genes. *Mol. Cell. Endocrinol.* **275**, 79–97 (2007).
23. Mosser, D.M. & Edwards, J.P. Exploring the full spectrum of macrophage activation. *Nat. Rev. Immunol.* **8**, 958–969 (2008).

24. Feng, X. *et al.* Lipopolysaccharide inhibits macrophage phagocytosis of apoptotic neutrophils by regulating the production of tumour necrosis factor alpha and growth arrest-specific gene 6. *Immunology* **132**, 287–295 (2011).
25. Nishi, C., Toda, S., Segawa, K. & Nagata, S. Tim4- and MerTK- mediated engulfment of apoptotic cells by mouse resident peritoneal macrophages. *Mol. Cell. Biol.* **34**, 1512–1520 (2014).
26. Seitz, H.M., Camenisch, T.D., Lemke, G., Earp, H.S. & Matsushima, G.K. Macrophages and dendritic cells use different Axl/Mertk/Tyro3 receptors in clearance of apoptotic cells. *J. Immunol.* **178**, 5635–5642 (2007).
27. Miksa, M., Komura, H., Wu, R., Shah, K.G. & Wang, P. A novel method to determine the engulfment of apoptotic cells by macrophages using pHrodo succinimidyl ester. *J. Immunol. Methods* **342**, 71–77 (2009).
28. Oka, K. *et al.* Lectin-like oxidized low-density lipoprotein receptor 1 mediates phagocytosis of aged/apoptotic cells in endothelial cells. *Proc. Natl. Acad. Sci. USA* **95**, 9535–9540 (1998).
29. Park, D. *et al.* BAI1 is an engulfment receptor for apoptotic cells upstream of the ELMO/Dock180/Rac module. *Nature* **450**, 430–434 (2007).
30. Schroeder, G.M. *et al.* Discovery of N-(4-(2-amino-3-chloropyridin-4-yloxy)-3-fluorophenyl)-4-ethoxy-1-(4-fluorophenyl)-2-oxo-1,2-dihydropyridine-3-carboxamide (BMS-777607), a selective and orally efficacious inhibitor of the Met kinase superfamily. *J. Med. Chem.* **52**, 1251–1254 (2009).
31. Lemmon, M.A. & Schlessinger, J. Cell signaling by receptor tyrosine kinases. *Cell* **141**, 1117–1134 (2010).
32. Kahn, C.R., Baird, K.L., Jarrett, D.B. & Flier, J.S. Direct demonstration that receptor crosslinking or aggregation is important in insulin action. *Proc. Natl. Acad. Sci. USA* **75**, 4209–4213 (1978).
33. Schreiber, A.B., Libermann, T.A., Lax, I., Yarden, Y. & Schlessinger, J. Biological role of epidermal growth factor-receptor clustering. Investigation with monoclonal anti-receptor antibodies. *J. Biol. Chem.* **258**, 846–853 (1983).
34. Todt, J.C., Hu, B. & Curtis, J.L. The receptor tyrosine kinase MerTK activates phospholipase C gamma2 during recognition of apoptotic thymocytes by murine macrophages. *J. Leukoc. Biol.* **75**, 705–713 (2004).
35. O'Bryan, J.P., Fridell, Y.W., Koski, R., Varnum, B. & Liu, E.T. The transforming receptor tyrosine kinase, Axl, is post-translationally regulated by proteolytic cleavage. *J. Biol. Chem.* **270**, 551–557 (1995).
36. Costa, M., Bellosta, P. & Basilico, C. Cleavage and release of a soluble form of the receptor tyrosine kinase ARK in vitro and in vivo. *J. Cell. Physiol.* **168**, 737–744 (1996).
37. Ekman, C., Site, D.F., Gottsater, A., Lindblad, B. & Dahlback, B. Plasma concentrations of growth arrest specific protein 6 and the soluble form of its tyrosine kinase receptor Axl as markers of large abdominal aortic aneurysms. *Clin. Biochem.* **43**, 110–114 (2010).
38. Zhu, H. *et al.* Different expression patterns and clinical significance of mAxl and sAxl in systemic lupus erythematosus. *Lupus* **23**, 624–634 (2014).
39. Ko, C.P., Yu, Y.L., Hsiao, P.C., Yang, S.F. & Yeh, C.B. Plasma levels of soluble Axl correlate with severity of community-acquired pneumonia. *Mol. Med. Rep.* **9**, 1400–1404 (2014).
40. Liu, X. *et al.* Plasma concentrations of sAxl are associated with severe preeclampsia. *Clin. Biochem.* **47**, 173–176 (2014).
41. Lee, C.H. *et al.* Plasma concentrations predict aortic expression of growth-arrest-specific protein 6 in patients undergoing coronary artery bypass grafting. *PLoS ONE* **8**, e79452 (2013).
42. Hsiao, F.C. *et al.* Circulating growth arrest-specific 6 protein is associated with adiposity, systemic inflammation, and insulin resistance among overweight and obese adolescents. *J. Clin. Endocrinol. Metab.* **98**, E267–E274 (2013).
43. Camenisch, T.D., Koller, B.H., Earp, H.S. & Matsushima, G.K. A novel receptor tyrosine kinase, Mer, inhibits TNF-alpha production and lipopolysaccharide-induced endotoxic shock. *J. Immunol.* **162**, 3498–3503 (1999).
44. Sen, P. *et al.* Apoptotic cells induce Mer tyrosine kinase-dependent blockade of NF-κB activation in dendritic cells. *Blood* **109**, 653–660 (2007).
45. Casanova-Acebes, M. *et al.* Rhythmic modulation of the hematopoietic niche through neutrophil clearance. *Cell* **153**, 1025–1035 (2013).
46. Scheiermann, C., Kunisaki, Y. & Frenette, P.S. Circadian control of the immune system. *Nat. Rev. Immunol.* **13**, 190–198 (2013).
47. Holland, S.J. *et al.* R428, a selective small molecule inhibitor of Axl kinase, blocks tumor spread and prolongs survival in models of metastatic breast cancer. *Cancer Res.* **70**, 1544–1554 (2010).
48. Ye, X. *et al.* An anti-Axl monoclonal antibody attenuates xenograft tumor growth and enhances the effect of multiple anticancer therapies. *Oncogene* **29**, 5254–5264 (2010).
49. Rothlin, C.V. & Lemke, G. TAM receptor signaling and autoimmune disease. *Curr. Opin. Immunol.* **22**, 740–746 (2010).
50. van den Brand, B.T. *et al.* Therapeutic efficacy of Tyro3, Axl, and Mer tyrosine kinase agonists in collagen-induced arthritis. *Arthritis Rheum.* **65**, 671–680 (2013).

ONLINE METHODS

Mice. The *Tyro3*$^{-/-}$, *Axl*$^{-/-}$, and *Mertk*$^{-/-}$ strains[9] and the *Gas6*$^{-/-}$ strain[51] were as published before. All lines, except for the TAM TKOs, have been back-crossed for >9 generations to a C57BL/6 background. All animal procedures were conducted according to guidelines established by the Salk Institutional Animal Care and Use Committee. Mice (8–12 weeks of age, both males and females) were randomly allocated to experimental groups (three to five mice per group) and investigators were blinded to group allocation during the experiment. Investigators were not blinded to sample identity. Group size was based on previous literature.

Reagents and antibodies. Dexamethasone, hydrocortisone, cortisone, aldosterone, 17β-estradiol, estrone, estriol, progesterone, DMSO and β-1,3-glucan from *Euglena gracilis* were from Sigma-Aldrich. CellTracker Orange (CMRA) was from Life Technologies. Pam3CSK4, HKLM, poly(I:C), LPS from *Escherichia coli*, ST-FLA, FSL-1, gardiquimod, CpG, MDP, iE-DAP and ppp-dsRNA-Lyo vector were from Invivogen. LPS from *Salmonella minnesota* R595 was from List Biological Laboratories. LPS for *in vivo* use was from *E. coli* serotype O55:B5 (Enzo). Mouse cytokines were IL-4 (Cell Signaling), TNF (Cell Signaling), IFN-α11 (PBL), IFN-β (PBL), IFN-γ (BioVision). Purified human protein S was from Haematologic Technologies. T0901317, GW501516, BRL49653 were provided by R. Evans. BMS-777607 was from Selleck Chemicals. Recombinant mouse GAS-6 was produced as published[10].

Antibodies used were as follows: anti-Mer (AF591), anti-Axl (AF854 or MAB854 (107332), used for costaining with Mer or Gas6), anti-GAS-6 (AF986) and anti-protein S (AF4036; all from R&D Systems); anti-Axl for immunoprecipitation (M-20) and anti-TYRO3 (C-20; sc-1095; both from Santa Cruz); anti-GAPDH (MAB374; 6C5) and antibody to phosphorylated tyrosine (4G10; both from Millipore); and antibody to phosphorylated NF-κB subunit p65 (3033; clone 93H1), anti-NF-κB (4764; C22B4), anti-STAT1 (9172), anti-Akt (4691; C67E7), antibody to phosphorylated Akt (4058; 193H12), anti-Erk1/2 (4695; 137F5), antibody to phosphorylated Erk1/2 (9101), anti-p38 (8690; D13E1) and antibody to phosphorylated p38 (4511; D3F9; all from Cell Signaling); and anti-CD68 (MCA1957; AbD Serotec), anti-CD11c (N418; eBioscience) and anti-CD11b (M1/70; eBioscience). The secondary antibodies used for immunoblot analysis were horseradish peroxidase–conjugated anti-goat (705-035-003; Jackson ImmunoResearch), anti-mouse (NA931V; GE Healthcare) and anti-rabbit (NA934V; GE Healthcare). The secondary antibodies for immunohistochemistry and immunocytochemistry were fluorophore-conjugated anti-goat (A-11055 (Life Technologies) or 705-166-147 (Jackson ImmunoResearch)) and anti-rat (712-606-153, 712-165-153 and 712-545-153; all from Jackson ImmunoResearch). The specificity of antibodies to Axl, Mer, TYRO3 and GAS-6 for immunohistochemistry, immunocytochemistry, immunoprecipitation and immunoblot analysis was assessed with samples from the respective genetically deficient mice (for example, **Figs. 1a** and **5g** and **Supplementary Fig. 2b**,**c**).

BMDM and BMDC cultures. Bone marrow cell cultures were differentiated as published before for BMDMs[52] and BMDCs[16]. Tibias and femurs from 6- to 8-week-old mice were flushed with sterile Dulbecco's PBS (Mediatech), and red blood cells were lysed with ACK lysis buffer (Lonza). For BMDMs, bone marrow cells were plated on Petri dishes in DMEM (Mediatech) supplemented with 10% FBS (SAFC Biosciences), PenStrep and 20% L929 supernatant. Fresh differentiation media was added on day 4. On day 7, macrophages were washed once with DPBS and split by scraping with a cell scraper. Cells were plated in DMEM with 10% FBS to allow adhesion. Once the cells attached, the media was changed to fresh serum-free media before experiments. For BMDCs, bone marrow cells were plated on 6-well plates in RPMI (Mediatech) supplemented with 5% FBS, 20 ng/ml mouse GM-CSF (Akron Biotech) and antibiotic-antimycotic 'cocktail' (Invitrogen). Fresh differentiation media was added on day 4. On day 7, DC aggregates were dislodged by being gently pipetted over the adherent stroma. Dislodged cells were pooled and resuspended in serum-free RPMI before experiments.

Cell stimulation with TAM ligands and activating antibodies. For TAM receptor activation, BMDM or BMDC cultures were incubated with serum-free medium for 18 h with or without addition of the appropriate stimuli. Cells were then stimulated with the appropriate concentration of recombinant mouse GAS-6, purified human protein S or activating antibodies for 10–30 min, and then were lysed for protein isolation. The TAM-activating antibodies were polyclonal anti-Axl (AF854), anti-Mer (AF591) and anti-TYRO3 (AF759; all from R&D Systems).

Immunoblot analysis and immunoprecipitation. BMDM and BMDC cultures were washed with ice-cold DPBS and were lysed on ice in a buffer containing 50 mM Tris-HCl pH 7.5, 1 mM EGTA, 1 mM EDTA, 1% Triton X-100, 0.27 M sucrose, 0.1% β-mercaptoethanol, and protease and phosphatase inhibitors (Roche). Tissues were 'snap frozen' in liquid nitrogen before lysis. For immunoblot analysis, equal amounts of protein (10 μg) in LDS sample buffer (Invitrogen) were separated by electrophoresis through 4–12% Bis-Tris polyacrylamide gels (Novex, Life Technologies) and were transferred to PVDF membranes (Millipore). For immunoprecipitation, cell lysates were incubated overnight at 4 °C with antibodies (0.2 μg antibody (identified above) for 0.5 mg protein in cell lysate). Protein G–Sepharose (Invitrogen) was added for 2 h and immunoprecipitates were washed twice with 1 ml of lysis buffer containing 0.5 M NaCl and once with 1 ml of 50 mM Tris-HCl pH 7.5. Immunoprecipitates were eluted in LDS buffer, separated by electrophoresis through polyacrylamide gels and transferred to PVDF membranes. Nonspecific binding was blocked with TBST (50 mM Tris-HCl pH 7.5, 0.15 M NaCl and 0.25% Tween-20) containing 5% BSA, and membranes were incubated overnight at 4 °C with primary antibodies (identified above) diluted 1,000-fold in blocking buffer. Blots were then washed in TBST and incubated for 1 h at 22–24 °C with secondary horseradish peroxidase–conjugated antibodies (identified above) diluted 5,000-fold in 5% skim milk in TBST. After repeating the washes, signal was detected with enhanced chemiluminescence reagent.

Enzyme-linked immunosorbent assay. Enzyme-linked immunosorbent assay for measurement of TNF (eBiosciences) and GAS-6 (R&D Systems) was done according to manufacturers' instructions.

Surface biotinylation. Cell surfaces were biotinylated as described[53]. Cells were washed three times with ice-cold PBS, pH 8.0, and were incubated for 30 min at 4 °C with 1 mg/ml Sulfo-NHS-LC-Biotin (Thermo) in PBS, pH 8.0. Cells were then washed three times with ice-cold 100 mM glycine in PBS and lysed.

Immunocytochemistry and immunohistochemistry. For immunohistochemistry, tissues were fresh frozen and cut into sections 11 μm in thickness, air-dried and stored desiccated at −70 °C. Before being stained, sections were fixed for 3 min with ice-cold acetone and washed in PBS, then nonspecific binding was blocked by incubation for 1 h in blocking buffer (PBS containing 0.1% Tween-20, 5% donkey serum and 2% IgG-free BSA). Slides were then washed in 0.1% Tween-20 in PBS and incubated overnight at 4 °C with 1 μg/ml primary antibody (identified above) in blocking buffer. Slides were then washed five times 5 min in PBS 0.1% Tween-20 and were incubated for 2 h at 22–24 °C in the dark with Hoechst and fluorophore-coupled donkey (Jackson) secondary antibodies (identified above) diluted 1:400 in blocking buffer. Slides were washed, sealed with Fluoromount-G (SouthernBiotech) and stored at 4 °C. For immunocytochemistry cells were plated on coverslips and treated with the appropriate stimuli. For fixed labeling, cells were first fixed for 10 min in 4% PFA and washed with PBS. Nonspecific binding was then blocked by incubation of coverslips for 30 min in blocking buffer with 0.1% Triton X-100; coverslips were washed in 0.1% Tween-20 in PBS and were incubated for 1 h at 22–24 °C with 1 μg/ml primary antibody (identified above). Coverslips were washed five times in PBS 0.1% Tween-20 and were incubated for 1 h at 22–24 °C in the dark with Hoechst stain and fluorophore-coupled donkey secondary antibody (identified above) diluted 1:400 in blocking buffer. Coverslips were washed and mounted on slides with Fluoromount-G. For live labeling, cells were incubated for 30 min at 4 °C with primary antibody (identified above) diluted to 1 μg/ml in cold medium. Cells were washed three times with cold DPBS and fixed for 10 min with 4% PFA. Nonspecific binding was blocked and coverslips incubated with secondary antibodies, washed and mounted as above. Images were obtained with a Zeiss LSM 710 microscope with Plan-Apochromat 20×/0.8 M27 and 63×/1.40

Oil DIC M27 objectives at the Salk Waitt Advanced Biophotonics Center Core Facility.

Scanning electron microscopy. Cells on coverslips were fixed overnight at 4 °C in 3% glutaraldehyde and 3% paraformaldehyde in PBS, pH 7.5. Samples were then dehydrated in a graded ethanol series on ice. After dehydration, the coverslips were loaded into Teflon sample holders and processed in an automated critical point drier (Leica EM CPD300; Leica), which was set to perform 25 exchange cycles of CO_2 at medium speed and 20% stirring. All additional fill, heating, and venting steps were performed at medium speed as well. After drying, the coverslips were carefully removed and were made to adhere to double-sided carbon tabs on aluminum stubs. The mounted samples were then 'sputter coated' (Leica SCD500; Leica) with approximately 7 nm of platinum while being rotated. Samples were then imaged on a scanning electron microscope (EVO HD, Zeiss Ltd.) at 3 kV for optimal contrast. The entire procedure was performed at the Waitt Advanced Biophotonics Center Core Facility, Salk Institute.

RT-qPCR. Total cellular RNA was isolated with an RNeasy Mini Kit according to the manufacturer's instructions (Qiagen). DNA was removed by on-column digestion with DNase (Qiagen). An RT Transcriptor First Strand cDNA Synthesis Kit (Roche) with anchored oligo(dT) primers (Roche) was used for reverse transcription. Quantitative PCR was run in a 384-well plate format on a ViiA 7 Real-Time PCR System (Applied Biosystems) with 2× SYBR Green PCR Master Mix (Applied Biosystems). Primers are in **Supplementary Table 1**. Expression was analyzed by the threshold cycle (ΔCt) method.

Phagocytosis assay. Differentiated BMDMs were plated on a 48-well plate at 70% confluency and were incubated for 24 h in DMEM containing indicated stimuli. For the generation of apoptotic cells, thymocytes were isolated from 3- to 6-week-old mice, red blood cells were lysed with ACK buffer and remaining cells were incubated for 6 h in RPMI medium containing 5% FCS and 2 μM Dex to induce apoptosis. This routinely resulted in 70% apoptotic and ≤5% necrotic cells. Apoptotic cells were then stained for 30 min with 100 ng/ml pHrodo-SE (Invitrogen) as published[27]. Labeled cells were washed twice in PBS containing 1% BSA (to block remaining pHrodo-SE) and 1 mM EDTA (to remove any bound GAS-6 and protein S) and once with DMEM. Apoptotic cells were then incubated for 10 min with recombinant mouse GAS-6 or purified human protein S and were added to macrophages at a ratio of 10:1 (apoptotic cells/phagocytes) and were incubated for 1 h at 37 °C. BMDMs were then briefly washed in DPBS and were incubated for 10 min at 37 °C in trypsin (0.25%), then were placed on ice and detached by vigorous pipetting. Phagocytosis was assessed by flow cytometry with post-acquisition data analysis with FlowJo software (TreeStar). pHrodo fluorescence was measured with excitation at 561 nm and emission filters for phycoerythrin (574-590 nm) on an LSR II (BD Biosciences) at the Flow Cytometry Core of the Salk Institute. For *in vivo* phagocytosis assay, pHrodo-labeled apoptotic cells were injected intraperitoneally. After 1 h peritoneal cavity was washed with ice cold PBS and the percent of $CD11b^+pHrodo^+$ phagocytic macrophages was quantified by flow cytometry.

Activating antibodies *in vivo*. Male 8- to 12-week-old mice were given intravenous injection (retro-orbital injection, 0.2 ml final volume) or intraperitoneal injection (0.3 ml final volume) of the appropriate concentration of activating antibody to Axl (AF854; R&D Systems) or to Mer (AF591; R&D Systems) or control IgG (AB-108-C; R&D Systems). Mice were killed at specified time points after injection and tissues were 'snap frozen' in liquid nitrogen for further analysis of protein and mRNA.

Data analysis. All experiments were done in duplicate or triplicate and were repeated at least three times. Replicate numbers were chosen to be adequate for the statistical method used. Data had normal distribution and equal variance. A two-tailed Student's *t*-test was used for statistical analysis. Differences with a P value of <0.05 were considered statistically significant.

51. Angelillo-Scherrer, A. *et al*. Deficiency or inhibition of Gas6 causes platelet dysfunction and protects mice against thrombosis. *Nat. Med.* **7**, 215–221 (2001).
52. Zhang, X., Goncalves, R. & Mosser, D.M. The isolation and characterization of murine macrophages. *Curr. Protoc. Immunol.* **83**, 14.1 (2008).
53. Fourgeaud, L. *et al*. The metabotropic glutamate receptor mGluR5 is endocytosed by a clathrin-independent pathway. *J. Biol. Chem.* **278**, 12222–12230 (2003).

doi:10.1038/ni.2986